

Chapter 3

Present-day coccolith fluxes recorded in central eastern Mediterranean sediment traps and surface sediments*

Abstract – Two sediment traps were deployed in time series collection from November 1991 to August 1994 at 3000 m and 3500 m, respectively, above and below the oxygenated sea water/anoxic brine interface in Bannock Basin, central eastern Mediterranean. Here the coccolithophore flux and its contribution to the carbonate particulate flux is presented for the 3000 m trap, and compared with the record in eastern Mediterranean surface sediments. A marked seasonal variation is observed in the fluxes of total mass, total coccoliths and whole coccospheres, with flux maxima in late winter and spring. The annual coccolith flux of 1.0×10^{10} coccoliths $\text{m}^{-2} \text{yr}^{-1}$ measured in the deep waters of Bannock Basin is much lower than published data from most other oceanographic settings, even when corrected for the trap efficiency of about 23% calculated from the ^{230}Th flux. The biogenic and lithogenic fluxes are primarily controlled by coccolithophore production and Saharan dust input, respectively. The calculated coccolith and coccosphere settling rates estimated from the comparison of maximum pigment concentration in the surface ocean and arrival of maximum flux at 3000 m water depth ranged from 17 – 25 m day^{-1} for coccoliths and 100 m day^{-1} for coccospheres. At the study site, carbonate dissolution is a minor process at both the trap depth and at the sea floor in both oxic and anoxic conditions, and there is a high preservation of coccolith CaCO_3 . Coccolithophores are the main contributor to the biogenic carbonate flux, followed by thoracosphaerids. *Emiliana huxleyi* and *Florisphaera profunda* followed by *Syracosphaera*, *Helicosphaera carteri* and *Calcidiscus leptoporus* are the dominant species in the sediment trap and surface sediments.

3.1 Introduction

The eastern Mediterranean is an area with extremely oligotrophic or ultra-oligotrophic conditions (Berland et al., 1988; Dugdale and Wilkerson, 1988; Yacobi et al., 1995). Heterotrophic bacterial production is tightly coupled with primary production. In particular, 85% of the primary production in the eastern Mediterranean flows to the microbial food web (Turley, 1997). Phytoplankton populations are dominated by picoplankton (Li et al., 1993) with the bacterial biomass constituting about 50% of total algal biomass (Robarts et al., 1996). The central eastern Mediterranean is net phototrophic, resulting in a sink for atmospheric CO_2 . Although eastern Mediterranean primary production estimates are generally low (Dugdale and Wilkerson, 1988), however, so far no one has studied how the productivity changes over the annual cycle in detail.

Coccolithophores are pelagic unicellular algae that secrete calcite plates. They are a

* This chapter has been published as: P. Ziveri, A. Rutten, G.J. de Lange, J. Thomson and C. Corselli, 2000, *Palaeogeography, Palaeoclimatology, Palaeoecology*, 158, 175-195.

major constituent of marine phytoplankton and make the major contribution to the biogenic carbonate content in deep-sea sediments (Bernard & Lecal, 1953; Milliman and Muller, 1973; Milliman, 1993). With their fast turnover, coccolithophores may have an important effect on the CO₂ cycle in the global ocean. They influence the global climate system through the organic carbon and carbonate pumps and by the emission of dimethyl sulfide which may affect cloud albedo (Andreae, 1986; Matrai and Keller, 1993; Charlson et al., 1987; Westbroek et al., 1993). Satellite imagery by the Coastal Zone Color Scanner (CZCS) revealed the formation of extensive blooms of the coccolithophore *Emiliana huxleyi* at higher latitudes in cooler, nutrient-rich waters (Holligan et al., 1983, Balch, 1997; Brown and Yoder, 1994). A better understanding of coccolithophore ecology is further required to use them as a biotic proxy of past climate change and to assess the quality and accuracy of the information preserved in the sediment record.

In the central eastern Mediterranean, coccolithophores are the dominant phytoplankton group that produces carbonate (Ziveri et al., 1995). In this study, we concentrate on the coccolithophore flux (number m⁻² day⁻¹) and its seasonality. In addition, annual fluxes will be compared with those estimated for nearby surface sediments. Present-day coccolithophore fluxes in the eastern Mediterranean have been measured by two automated sediment traps capable of collecting particles for specified time intervals over a long period.

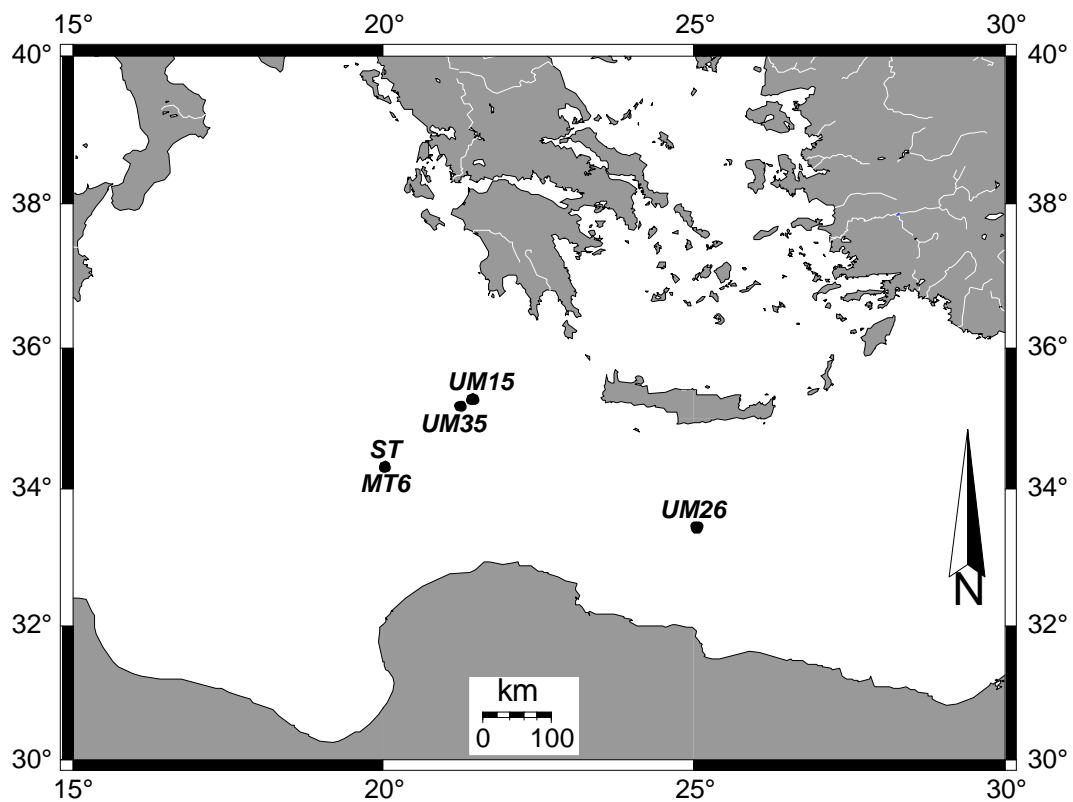


Figure 3.1 Map of the central eastern Mediterranean showing the locations of the sediment trap mooring (ST) and boxcores (MT6, UM15, UM35 and UM26) used in this study.

3.2 Material and methods

Two time-series sediment traps (Technicap PPS5/2) were deployed in the southwestern Bannock Basin (Libeccio subbasin; 34°18'N; 20°01'E), a central eastern Mediterranean anoxic basin (Scientific staff of Cruise Bannock 1984-12, 1985) (Fig. 3.1). Collection was from November 1991 until August 1994. During the 927-day deployment, each sediment trap opened and closed 96 times, providing a near-continuous time-series (Table 3.1). The upper trap was located at 3000 m, above the sea-water / brine interface in oxygenated conditions, whereas the lower trap, at 3500 m, was located in anoxic brine close to the bottom of Libeccio Basin (Fig. 2.2 in Chapter 2). Samples 21, 22, 23 (from 20-04-1992 to 05-05-1992) collected by the trap at 3000 m were empty, whereas sample 24 was unusually large, but no technical failure was apparent. In addition, a high mass flux was recorded in the anoxic trap at the same time in the synchronous sample 24. For this reason, we include all samples in all calculations.

A detailed description of the deployment and recovery of the sediment traps, sample additives, integrity and analytical methods are reported in Chapter 2 and by Ziveri et al. (1995). Sediment trap efficiency was evaluated using the flux of the long-lived radionuclide ^{230}Th (Chapter 2).

The surface sediment of four eastern Mediterranean boxcores, from 2160 – 3520 m water depth, were analysed for comparison with the accumulation rates and taxonomic composition of the coccolithophores estimated from the traps (Fig. 3.1, Table 3.2).

3.2.1 Coccolithophore sediment trap sample preparation

All samples were split on recovery on board ship into equal fractions using a pneumatic splitter (Tennant and Baker, 1992). For coccolith analysis, the first three series of samples (1 – 72) were collected on board upon 0.45 μm cellulose acetate (samples 1 – 48: 47 mm diameter; samples 49 – 72: 25 mm diameter) using a gas pressure system. The final set of samples (73 – 96) were maintained in solution and then split and filtered in the laboratory of the Department of Biology, University of Milan. After stirring the solution, a small portion of the sample was collected using a precision pipette and filtered on to a 0.45 μm cellulose acetate filter (47 mm diameter).

Table 3.1 *Sediment trap mooring phases, sampling period per phase, sample interval and deployment days per sampling phase. Sediment trap position: 34°17.84'N 20°00.89'E. Sediment trap depth: 3000 m. Water depth: 3530 m.*

Mooring Phase	Phase Start date	Phase End date	Deployment (days)	Sample interval (days)
ST2	10 Nov 1991	10 May 1992	182.5	5–10
MT40	1 Jun 1992	19 Feb 1993	263	9–14
MU-B	1 Apr 1993	16 Sep 1993	168	7
UM1STO	20 Oct 1993	29 Aug 1994	313	10–20

Table 3.2 Boxcore position, sampling interval, water depth, type of sediment and data used for the calculation of the coccolith accumulation rates (excluding coccolith concentration). These data include the sedimentation rates (cm kyr^{-1}), dry bulk densities (g cm^{-3}), percent mass accumulation rates ($\text{mg cm}^{-2} \text{kyr}^{-1}$) and CaCO_3 content (%) of the surface sediments analysed in the present study. The sedimentation rates and the dry bulk densities are from Van Santvoort et al. (1996), excluding the data for MT6 (see Appendix 3-A).

Boxcore	Position (latitude, longitude)	Sampling Interval (cm)	Water Depth (m)	Sediment Type	Sed. Rate (cm kyr^{-1})	Dry Bulk Density (g cm^{-3})	Mass. Accum. Rate ($\text{g cm}^{-2} \text{kyr}^{-1}$)	Total CaCO_3 Weight (%)
UM15	35°17.39'N 21°24.82'E	0.0 – 1.0	3307	Oxic, homogenised	4.7	0.8	4.2	51.3
UM26	33°23.58'N 25°00.93'E	0.0 – 0.5	2160	Oxic, homogenised	2.7	0.8	2.6	53.7
UM35	35°11.04'N 21°12.54'E	0.0 – 1.0	2670	Oxic, homogenised	3.3	0.9	3.1	54.5
MT6	34°17.09'N 20°01.16'E	0.0 – 0.5	3520	Anoxic, laminated	14.1	0.2	6.1	37.7

For the coccolith analysis of samples 1 to 72, the material on the filter had to be resuspended off the filter. Each filter was put into a glass culture tube containing a known volume of filtered (0.2 μm) distilled water buffered with sodium borate. The solution was stirred for a few minutes to allow detachment of the material from the fiber filter. A portion (1/8 – 1/1000 of the original sample) of the solution was collected by precision pipette and refiltered on to a 0.45 μm cellulose acetate filter (47 mm diameter). A 1 to 2 mm^2 area of each filtered membrane was subsequently analysed using a polarised light optical microscope (LM) at 1250 \times magnification to determine the total coccolith, coccosphere and calcareous dinocyst fluxes and the fluxes of the individual coccolithophore species (Ziveri and Thunell, 2000). A larger area (about 30 mm^2) was then used to quantify fluxes of coccospheres and calcispheres of thoracosphaerids (calcareous dinocysts). A scanning electron microscope (SEM) was used to evaluate the sample preparation, the coccolithophore taxonomical composition and coccolith preservation. The flux results on the other major biogenic contributors will be given in Ziveri et al. (in prep.).

The evenness of the distribution of coccoliths across the filter surface was confirmed by quantifying their distribution on different areas across the filter on samples from different production episodes. An average of 709 (405 – 1302) coccoliths were counted per sample; the number of coccospheres counted per sample ranged from 0 – 340.

3.2.2 Coccolithophore surface sediment sample preparation

Total coccoliths per gram of dry sediment (coccoliths g^{-1}) and the coccolith taxonomic composition were determined in the <32 μm fraction from the top sediment of four boxcores (upper 0.5 to 1 cm) located close to the trap mooring (UM15, UM35, MT6) and at a more eastern site (UM26).

The <32 μm and 32 – 1000 μm fractions for each sample were obtained by wet sieving 0.25 – 0.5 g of freeze-dried sediment following the filtration method described in Lototskaja et al. (1998). Each size fraction was collected on to 0.45 μm Millipore filters (47 mm diameter) using prefiltered distilled water with a sodium borate buffer. A low-pressure vacuum pump was used for filtration in order to improve the even distribution of the particles on the filter. Each membrane was oven-dried at 40°C and stored in an air-tight container. Coccolithophore quantification was carried out on the <32 μm fraction; the >32 μm fraction was qualitatively analysed to evaluate the sieving efficiency. The weight percentage of the >32 μm and <32 μm size fractions for samples of UM15, UM26 and UM35 was obtained by wet-sieving 0.5 g sediment and subsequent oven drying.

The sedimentation rates (cm kyr^{-1}), dry bulk densities (g cm^{-3}), mass accumulation rates ($\text{mg cm}^{-2} \text{kyr}^{-1}$) and CaCO_3 content (wt%) of the surface sediments analysed in this study are presented in Table 3.2. The sedimentation rates and the dry bulk densities are from Van Santvoort et al. (1996), excluding the data for MT6 (see Appendix 3-A). The carbonate content of the fine fraction was determined by gasometric techniques, with a precision of $\pm 2\%$

Coccolith accumulation rates were calculated using the following formula (Lototskaya et al, 1998; Ziveri and Thunell, 2000):

$$\text{ARc} = \text{Dc} \times \text{DBD} \times \text{SR} \quad (1)$$

where AR_c is the coccolith accumulation rate (number of coccoliths $\text{cm}^{-2} \text{yr}^{-1}$), D_c the coccolith density (number of coccoliths g^{-1}), DBD the dry bulk density (g cm^{-3}), and SR the sedimentation rate (cm yr^{-1}).

The coccolith taxonomic composition of the top sediments was determined by LM in the same way as the trap samples and 500 specimens were counted for each; SEM was used to evaluate the preparation of the samples, the coccolith carbonate preservation and species diversity.

Taxonomic identification for the determination of the species diversity follows Ziveri et al. (1995). For quantification, all holococcoliths were classed as holococcolith spp., and the *Syracosphaera* group includes all *Syracosphaera* species excluding *S. pulchra* and *S. histrica*.

3.3 Results

3.3.1 Sediment trap

The seasonal pattern of coccolithophore deposition recorded in the 3000 m Bannock Basin sediment trap exhibits highest coccosphere fluxes during January – May 1992, April – May 1993 and January 1994, and highest individual coccolith fluxes during late March – mid July 1992, April – June 1993 and late October – January 1994 (Fig. 3.2). Maximum coccolith and coccosphere fluxes occur in April 1993, reaching values of 3.0×10^8 coccoliths $\text{m}^{-2} \text{day}^{-1}$ and 6.2×10^4 coccospheres $\text{m}^{-2} \text{day}^{-1}$, respectively. The contribution of intact coccospheres to the total coccolith flux is relatively small in comparison to the settling of individual coccoliths.

The coccolithophore flux peaks are caused mainly by an increased flux of *E. huxleyi* (Fig. 3.3). The taxonomic composition of the coccolithophore assemblages in the trap samples is dominated by *E. huxleyi* (on average 82.2% of the total coccolith assemblage; range between 6.3 and 95%) and secondarily by *F. profunda* (average 5.3%; range 0 – 50.4%), *Syracosphaera* (average 3.9%; range 0 – 31.9%) and *H. carteri* (average 3.1%; range 0 – 31.2%) (Fig. 3.3).

The fifty coccolithophore species identified in the sediment trap samples are listed in Table 3.3. The 500 specimens counted for each sample lead to a 95% probability level of detecting a species present in the population at 1%.

Maximum fluxes of thoracosphaerids are recorded during April till June 1992 and 1993, and from November 1993 to January 1994 and July to August 1994 (Fig. 3.2). The mean flux is 6.5×10^4 calcispheres $\text{m}^{-2} \text{day}^{-1}$.

Coccolithophores are the major contributor to the biogenic carbonate flux in Bannock Basin, and are also the dominant phytoplankton group detected in the trap samples (Ziveri et al., 1995). Calcareous dinoflagellates, mainly *Thoracosphaera hemii*, are the only additional calcareous component that contribute considerably to the biogenic carbonate fluxes (average of 17%). Foraminifers are present mainly as juvenile forms and have low fluxes. An increase in juvenile foraminifer flux has been recorded in July–August 1994 (Ziveri et al., in prep.).

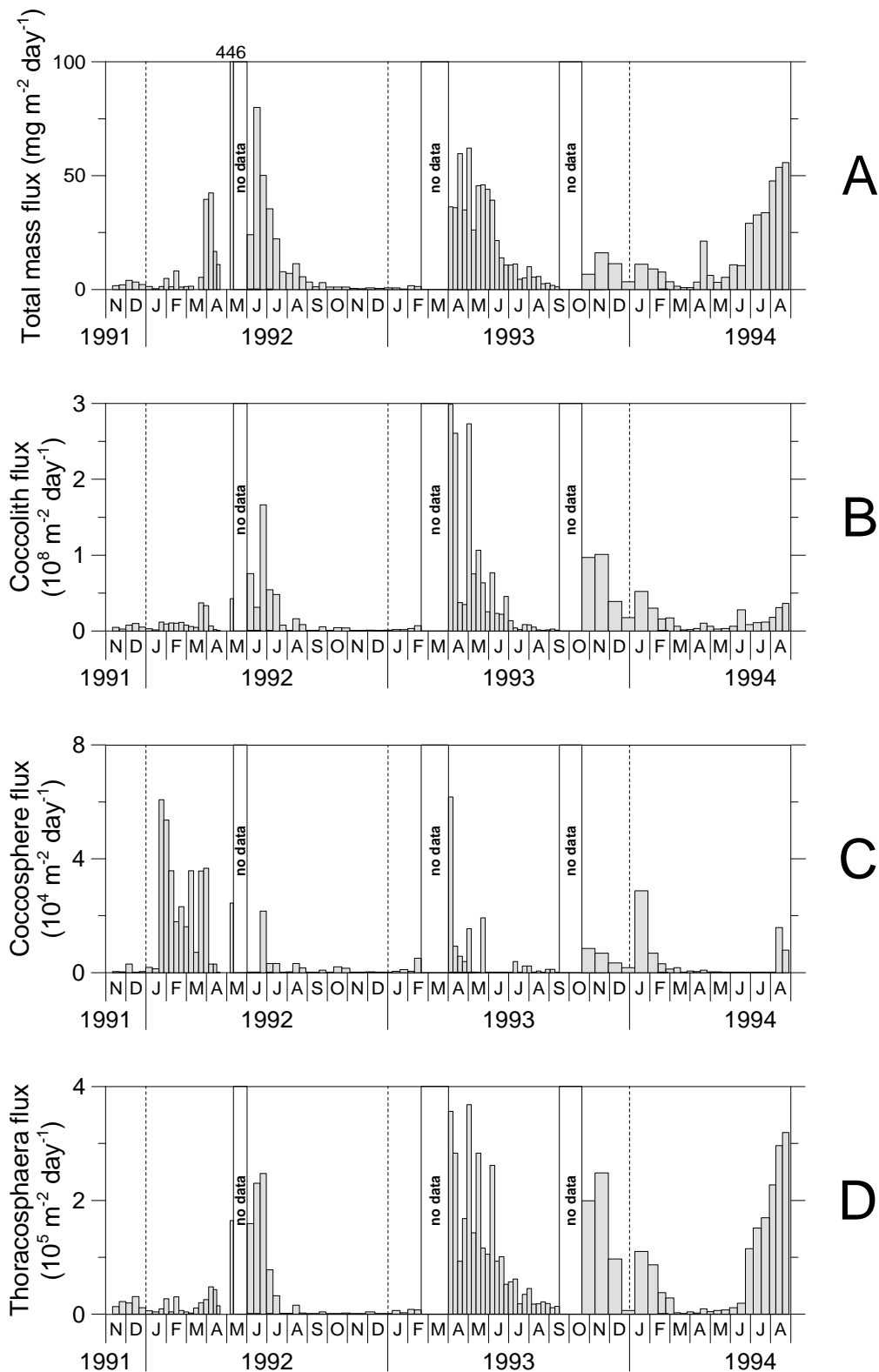


Figure 3.2 Flux records for: A) Total mass ($\text{mg m}^{-2} \text{day}^{-1}$); B) Total coccoliths ($\text{number m}^{-2} \text{day}^{-1}$); C) Cocospheres ($\text{number m}^{-2} \text{day}^{-1}$); D) Thoracosphaerids ($\text{number m}^{-2} \text{day}^{-1}$), at Bannock Basin at 3000 m water depth.

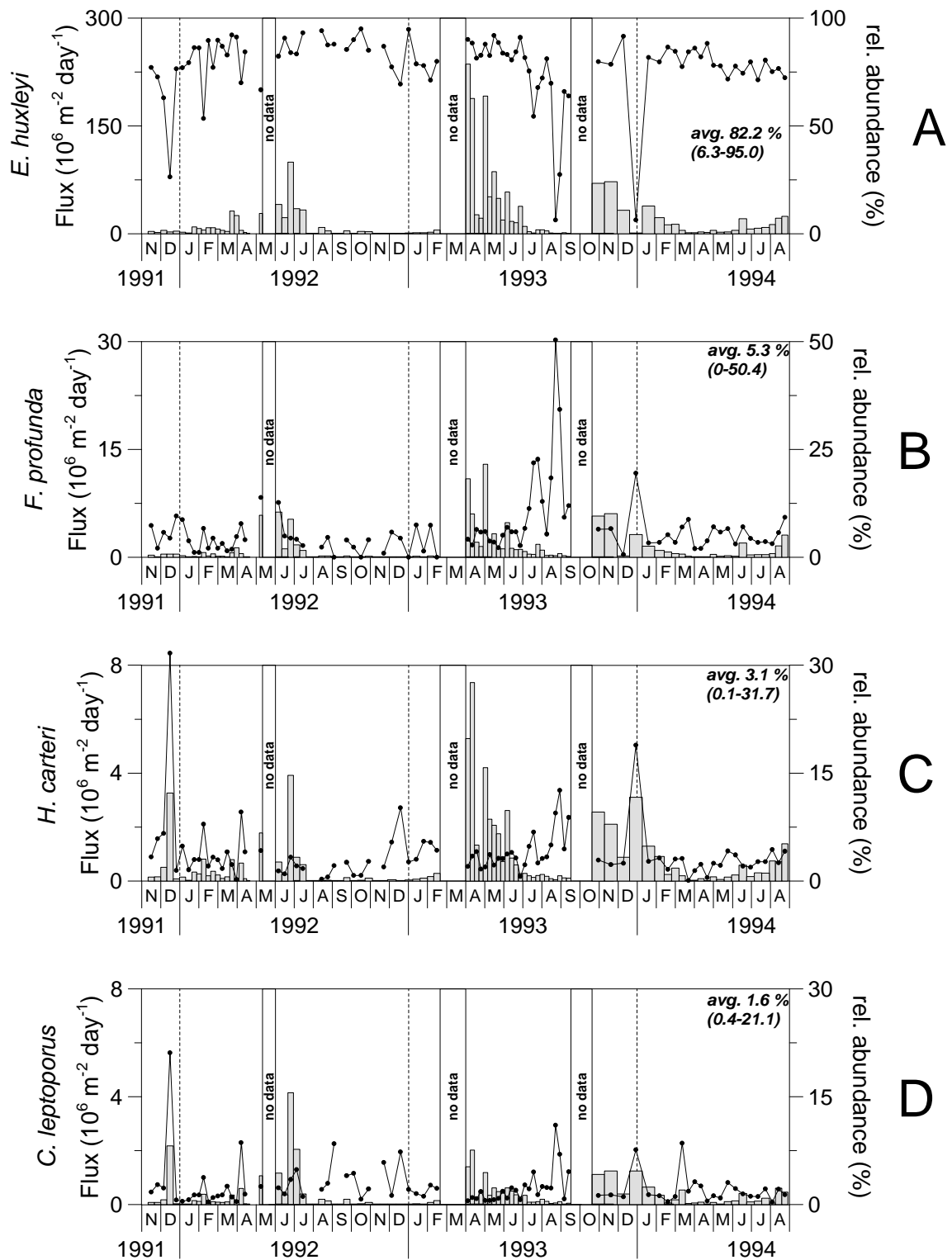


Figure 3.3 Coccolith flux ($\text{number m}^{-2} \text{ day}^{-1}$) (bars) and relative abundance (% of total coccolith flux) (lines) records of the major individual species of coccolithophores. The relative abundance is defined as flux of a certain species ($\text{number m}^{-2} \text{ day}^{-1}$) divided by total coccolith flux ($\text{number m}^{-2} \text{ day}^{-1}$) and multiplied by 100%.

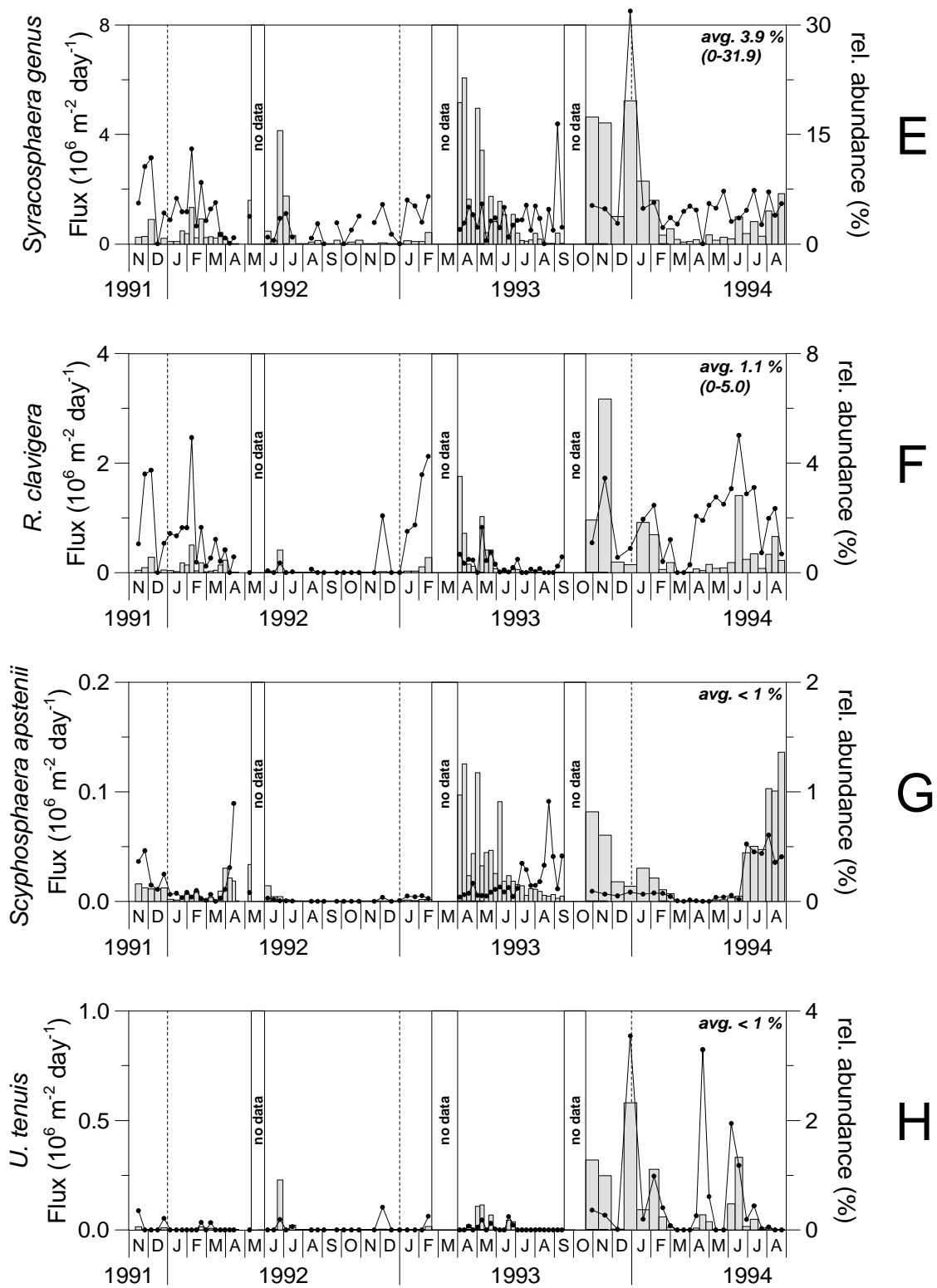


Figure 3.3 (continued)

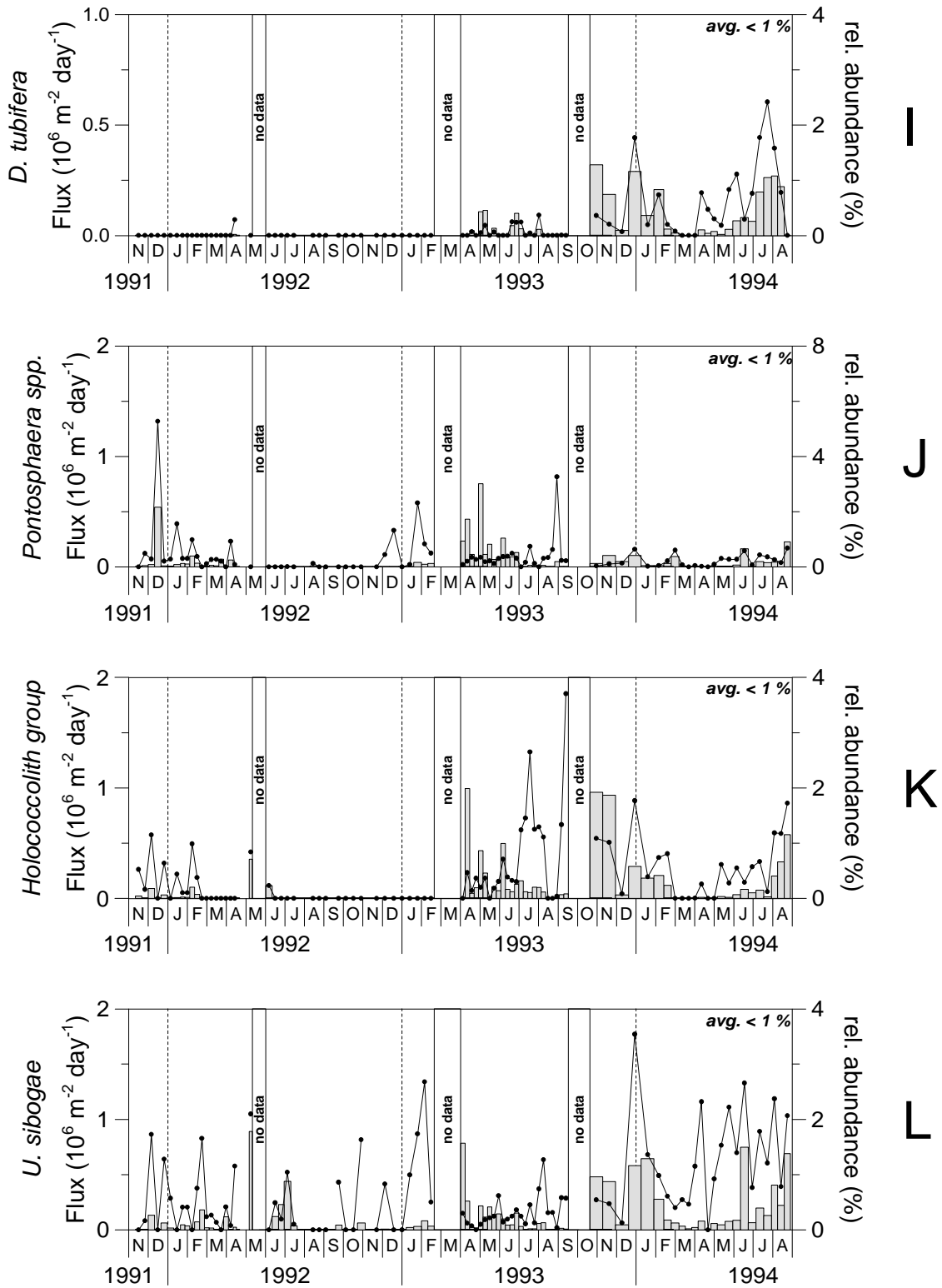


Figure 3.3 (continued)

3.3.2 Surface sediments

The Ca content of the surface sediments of boxcores UM15, UM26 and UM35 varies from 18 to 24 wt% and is 15 wt% for boxcore MT6, located in the anoxic brine basin. Higher annual coccolith accumulation rates were found in the anoxic surface sediments (core MT6) from Bannock Basin (Fig. 3.4; Table 3.4). The coccolith accumulation rates range from 2×10^{12} to 3.9×10^{13} coccoliths $\text{m}^{-2} \text{kyr}^{-1}$. *Emiliana huxleyi* dominates the sediment assemblage, followed by *F. profunda*, *H. carteri* and *C. leptoporus* (Fig. 3.4; Table 3.4).

3.4 Discussion

3.4.1 Seasonal trend of coccolithophore and thoracosphaerid fluxes

During the 3-year time series the mass flux pattern was characterised by low mass particle fluxes with an average of about $16 \text{ mg m}^{-2} \text{ day}^{-1}$. This value is several times lower than the average mass flux measured at 1000 m depth in the North Balearic Northwestern Mediterranean ($185\text{--}588 \text{ mg m}^{-2} \text{ day}^{-1}$), Adriatic sea ($341 \text{ mg m}^{-2} \text{ day}^{-1}$) and west of Crete ($46 - 210 \text{ mg m}^{-2} \text{ day}^{-1}$) (Heussner and Monaco, 1996), and in the Alboran Sea ($197 \text{ mg m}^{-2} \text{ day}^{-1}$; Dachs et al., 1986). It is, however, similar to the flux recorded in the western Mediterranean northwest of Corsica ($22 \text{ mg m}^{-2} \text{ day}^{-1}$; Miquel et al., 1994).

The total mass and coccolith fluxes recorded in Bannock Basin present a strong seasonal pattern with a general increase in late winter to early spring. The major component of the mass flux in the sediment trap appears to be of terrigenous origin (60 wt%) (Chapter 2). The average total carbonate content is relatively low (31.5 wt%) compared to those in the top sediments of the eastern Mediterranean. In contrast, the biogenic particle fluxes in the sediment trap at the Bannock Basin site are largely dominated by carbonate (~70%). Dilution of the biogenic components is, therefore, an important process. The dilution effect by terrigenous input is demonstrated by the general inverse trends of the Al flux (an indicator of terrigenous input) and the coccolith concentrations obtained by dividing coccolith flux by mass flux (Fig. 3.5).

Little work has been performed in the eastern Mediterranean on living coccolithophores and almost nothing is known about their spatial and temporal distribution or their export production to the sea floor. One previous investigation (Knappertsbusch, 1993) in the eastern Mediterranean in 1986 to 1988 registered a very high seasonal variability in coccolithophore production. The highest production was found in February to March, largely dominated by *E. huxleyi*. Preliminary results from the oligotrophic waters of the south Aegean Sea and the Straits of Cretan Arc show that coccolithophores were the dominant phytoplankton group in March and September (Balopoulos et al., 1996).

The annual coccolith flux of 1.0×10^{10} coccoliths $\text{m}^{-2} \text{yr}^{-1}$ measured in the deep waters of Bannock Basin is much lower than most published data recorded in other oceanographic settings ($10^{11} - 10^{12}$ coccoliths $\text{m}^{-2} \text{yr}^{-1}$; Steinmetz, 1991; Broerse et al., 2000; Haidar et al., 2000; Sprengel et al., 2000; Ziveri and Thunell, 2000). This result remains low even after we correct the value for the trap efficiency of 23% calculated from the ^{230}Th (Chapter 2).

Thoracosphaera fluxes parallel the mass flux ($r=0.72$). Data on thoracosphaerid fluxes

in the ocean still remain scarce. Their annual fluxes (2.4×10^7 calcispheres $\text{m}^{-2} \text{yr}^{-1}$) in Bannock Basin are higher than those recorded in open ocean Northeast Atlantic stations at $48^\circ\text{N}21^\circ\text{W}$ however, and are comparable to the data collected at $38^\circ\text{N} 21^\circ\text{W}$ (Broerse et al., 2000). Enhanced calcareous cyst production can be observed in regions and time intervals with stratified, oligotrophic conditions in the upper water masses (Höll et al., 1999; Zonneveld et al., 1999).

Table 3.3 List of the coccolithophore species recorded in the sediment trap (extrapolated by 926-day deployment) in Bannock Basin and sediment samples from Bannock Basin and the eastern Mediterranean. The relative abundances (%) of the main coccolithophore species in the sediment trap and surface sediments are shown in Table 3.4.

Species	Sediment Trap Bannock Basin (3000 m)	Surface Sediments			
		UM15 (3307 m)	UM26 (2160 m)	UM35 (2670 m)	MT6 (3520 m)
Heterococcolithophores					
1. <i>Algirosphaera oryza</i> Schlauder 1945	Yes	Yes	Yes	Yes	No
2. <i>Anopsolenia brasilianensis</i> (Lohmann 1919) Deflandre 1952	Yes	Yes	No	No	No
3. <i>Braarudosphaera bigelowi</i> (Gran and Braarud 1935) Deflandre 1947	Yes	No	No	No	No
4. <i>Calcidiscus leptoporus</i> (Murray and Blackmann 1898) Loeblich and Tappan 1978	Yes	Yes	Yes	Yes	Yes
5. <i>Ceratolithus cristatus</i> Kamptner 1950 var. <i>cristatus</i> <i>C. cristatus</i> var. <i>telesmus</i> (Norris 1965) Jordan and Young 1990	Yes Yes	No No	Yes No	No Yes	No No
6. <i>Coccolithus pelagicus</i> (Wallich 1877) Aciller 1930 f. <i>pelagicus</i>	Yes	No	No	No	Yes
7. <i>Coronosphaera mediterranea</i> (Lohmann 1902) Gaarder and Heimdal 1977	Yes	Yes	Yes	Yes	Yes
8. <i>C. binodata</i> (Kamptner 1927) Gaarder and Heimdal 1977	Yes	No	No	No	No
9. <i>Discosphaera tubifera</i> (Murray and Blackman 1989) Ostenfeld 1900	Yes	Yes	No	No	No
10. <i>Emiliania huxleyi</i> (Lohmann 1902) Hay and Mohler, in Hay et al. 1967	Yes	Yes	Yes	Yes	Yes
11. <i>Florisphaera profunda</i> Okada and Honjo 1973	Yes	Yes	Yes	Yes	Yes
12. <i>Gephyrocapsa caribbeanica</i> Boudreaux and Hay, in Hay et al. 1967	Yes	Yes	Yes	Yes	Yes
13. <i>G. ericsonii</i> McIntyre and Bé 1967	Yes	Yes	Yes	Yes	Yes
14. <i>G. ornata</i> Heimdal, 1973	Yes	No	No	No	No
15. <i>G. muelleriae</i> Breheret 1978 type A	Yes	Yes	Yes	Yes	Yes
16. <i>G. oceanica</i> Kamptner 1943	Yes	Yes	Yes	Yes	Yes
17. <i>Gladiolithus flabellatus</i> (Halldal and Markali 1955) Jordan and Chamberlain 1993	Yes	Yes	Yes	Yes	Yes
18. <i>Helicosphaera carteri</i> (Wallich 1978) Kamptner 1954	Yes	Yes	Yes	Yes	Yes
19. <i>H. pavementum</i> Okada and McIntyre 1977	Yes	No	Yes	No	No
20. <i>Neosphaera coccolithomorpha</i> Lecal-Schlauder 1950	Yes	No	No	No	Yes

Species	Sediment Trap	Surface Sediments			
		Bannock Basin (3000 m)	UM15 (3307 m)	UM26 (2160 m)	UM35 (2670 m)
21. <i>Oolithotus fragilis</i> (Lohman 1912) Okada and McIntyre 1977	Yes	Yes	Yes	Yes	No
22. <i>Ponthosphaera japonica</i> (Takayama 1967) Nishida 1971	Yes	No	Yes	No	No
23. <i>P. discopora</i> Schiller 1925	Yes	Yes	Yes	Yes	Yes
24. <i>P. syracusana</i> Lohmann 1902	Yes	Yes	No	No	No
25. <i>Reticulofenestra parvula</i> (Okada and McIntyre 1977) Biekart 1989	Yes	Yes	Yes	Yes	Yes
26. <i>Reticulofenestra</i> "overcalcified" sp.	Yes	Yes	Yes	Yes	Yes
27. <i>Rhabdosphaera clavigera</i> Murray and Blackman 1989	Yes	Yes	Yes	Yes	Yes
28. <i>R. xiphos</i> (Deflandre and Fert 1954) Norris 1984	Yes	No	No	No	No
29. <i>Scyphosphaera apstenii</i> Lohman 1902	Yes	No	No	No	Yes
30. <i>Syracosphaera anthos</i> (Lohman 1912) Jordan and Young 1990	Yes	Yes	No	No	No
31. <i>S. corrugis</i> Okada and McIntyre 1977	Yes	No	No	No	No
32. <i>S. halldalii</i> (Weber-van Bosse, 1901) Gaarder 1970	Yes	Yes	No	Yes	Yes
33. <i>S. histrica</i> Kamptner 1941	Yes	No	No	No	No
34. <i>S. pulchra</i> Lohmann 1902	Yes	Yes	Yes	Yes	Yes
35. <i>Umbellosphaera irregularis</i> Paashe, in Markali and Paashe 1955	Yes	No	No	No	No
36. <i>U. tenuis</i> (Kamptner 1937) Paashe, in Markali and Paashe 1955	Yes	Yes	Yes	Yes	Yes
37. <i>Umbilicosphaera hulburtiana</i> Gaarder 1970	Yes	No	No	No	No
38. <i>U. sibogae</i> (Weber-van Bosse 1901) Gaarder 1970	Yes	Yes	No	No	No
Holococcolithophores					
39. <i>Antosphaera fragaria</i> (Kamptner 1953) Kleijne 1991	Yes	No	No	No	No
40. <i>Calyptrolithina multipora</i> (Gaarder, in Heimdal and Gaarder 1980) Norris 1985	Yes	No	No	No	Yes
41. <i>C. wettsteinii</i> (Kamptner 1937) Kleijne 1991	Yes	Yes	Yes	No	No
42. <i>Calyptrolithophora papillifera</i> (Halldal 1953) Heimdal, in Heimdal and Gaarder 1980	Yes	No	No	No	Yes
43. <i>Calyptrosphaera oblonga</i> Lohmann 1902	Yes	Yes	No	Yes	Yes
44. <i>Calyptrosphaera pirus</i> Kamptner 1937	Yes	No	Yes	No	No
45. <i>Gliscolithus amitakarenae</i> Norris 1985	No	Yes	No	No	No
46. <i>Homozyso-sphaera vercellii</i> Borsetti and Cati, 1979	Yes	No	No	No	No
47. <i>S. dalmaticus</i> (Kamptner 1927) Loeblich and Tappan 1963	Yes	No	No	Yes	No
48. <i>S. quadriperforatus</i> (Kamptner 1937) Gaarder 1962	Yes	Yes	No	Yes	No
49. <i>Syracolithus confusus</i> Kleijne 1991	Yes	No	No	No	No
50. <i>Zygosphaera hellenica</i> Kamptner 1937	Yes	No	No	Yes	No

Table 3.4 Estimated annual coccolith flux (coccoliths $m^{-2} yr^{-1}$) in the sediment trap (extrapolated by 926-day deployment) and surface sediments, and relative abundances (%) of the main coccolithophore species in the sediment trap and surface sediments^a.

	Coccolith species abundance (%)				
	Sediment trap ^b	Boxcore UM15 ^c	Boxcore UM26 ^d	Boxcore UM35 ^e	Boxcore MT6 ^{f*}
<i>C. leptoporus</i>	1.61	<1	<1	<1	1.34
<i>D. tubifera</i>	<1	1.72	2.90	1.06	<1
<i>Reticulofenestra</i> “overcalcified” sp.	<1	4.58	31.10	19.84	3.32
<i>E. huxleyi</i>	82.22	68.19	28.10	57.14	55.52
<i>F. profunda</i>	5.28	9.16	12.98	5.17	9.03
<i>G. flabellatus</i>	<1	1.15	2.48	<1	<1
<i>G. oceanica</i>	<1	<1	<1	<1	1.34
<i>H. carteri</i>	3.06	<1	<1	<1	1.67
<i>N. coccolithomorpha</i>	<1	3.72	4.99	5.03	0.00
<i>Oolithothus</i> spp.	<1	<1	1.14	<1	<1
<i>R. clavigera</i>	1.07	<1	<1	2.38	0
<i>R. xiphos</i>	<1	2.01	2.17	1.85	0
<i>S.pulchra</i>	<1	<1	2.57	1.59	<1
<i>Syracosphaera</i> spp.	3.92	1.15	1.29	<1	1.67
<i>S. fossilis</i>	<1	2.01	1.63	<1	0
<i>U. tenuis</i>	<1	1.15	1.61	<1	1
<i>U. sibogae</i>	<1	<1	2.03	<1	1
Holococcoliths	<1	<1	2.41	1.32	<1

^a MT6 = boxcore located in anoxic environment.

^d Annual coccolith flux (number per $m^{-2} y^{-1}$) = 2.31×10^9 .

^b Annual coccolith flux (number per $m^{-2} y^{-1}$) = 1.0×10^{10} .

^e Annual coccolith flux (number per $m^{-2} y^{-1}$) = 5.87×10^9 .

^c Annual coccolith flux (number per $m^{-2} y^{-1}$) = 1.0×10^{10} .

^f Annual coccolith flux (number per $m^{-2} y^{-1}$) = 3.9×10^{10} .

3.4.2 Factors controlling the temporal and spatial variability of coccolithophores, and the transfer processes to the deep Mediterranean waters

The particle flux in the ocean is mainly controlled by biological processes, occurring in the upper ocean, and by eolian and riverine input. Our work suggests that, in the central eastern Mediterranean, these two main particle flux sources of biogenic and lithogenic origin are primarily controlled by coccolithophore production and Saharan dust input, respectively.

Satellite derived, 7-year average (1979 – 1985), monthly surface pigment concentrations were estimated using data collected by the Coastal Zone Color Scanner (CZCS) (courtesy of the Joint Research Centre, European Commission/European Space Agency) and show an annual variation in primary production (Fig. 3.6). The pigment concentration record is used as a proxy for surface primary productivity and is very similar from year to year. In the eastern Mediterranean, the overall pigment concentrations are low when compared to other oceanic basins, even during the high-productivity season, and most of the production occurs in the period from December to March.

Sea surface temperatures (SST) were derived from Advanced Very High Resolution Radiometer (AVHRR) data for the study period (November 1991 to August 1994) and have

been generated using weekly composite AVHRR data for the Bannock Basin trap location (Fig. 3.6). The sea surface temperature varies between 15 and 28°C at Bannock Basin, with highest temperatures in summer and fall (Fig. 3.6). The average SST in the summer and winter of 1994 appears to be 1°C higher than those in 1992 and 1993.

Massive airborne plumes of desert dust from Sahara are exported to the Mediterranean all year long (Bergametti et al., 1989; Moulin et al., 1997). Although dust concentrations in the Mediterranean atmosphere and chlorophyll concentrations correlate negatively, there are differences between the dry and wet dust deposition. In the Mediterranean, wet dust deposition contributes 65 – 80% to the total dust deposition (Molinaroli et al., 1993). Because precipitation only occurs in winter, most of the yearly dust deposition to the sea water occurs in this period. A relationship between dust input and primary production was shown by the results of the Ironex II program, which established physiological limitation of phytoplankton

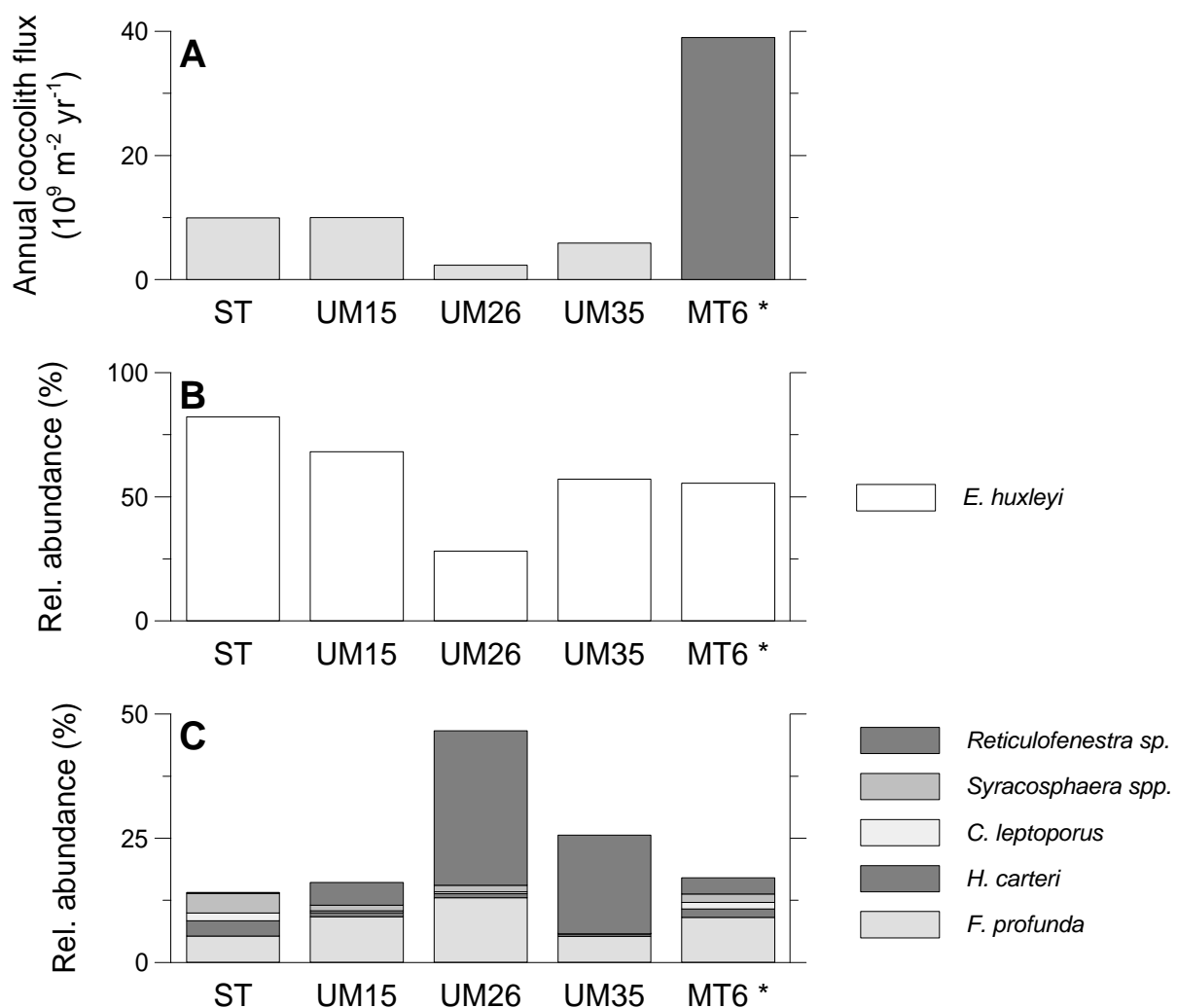


Figure 3.4 Comparison of sediment trap (ST) and surface sediment (boxcores MT6, UM15, UM35 and UM26) results: A) Annual coccolith flux (number $\text{m}^{-2} \text{ yr}^{-1}$); B) Relative abundance (%) of *E. huxleyi*; C) Relative abundance (%) of the major coccolith species excluding *E. huxleyi*.

by iron as the cause of the high nutrient, low chlorophyll phenomenon at eastern equatorial Pacific Ocean (Martin et al., 1994; Behrenfeld et al., 1996). We are aware of the fact that phosphorus, not iron, is the limiting nutrient in the eastern Mediterranean (Krom et al., 1991; Zohary and Robarts, 1998), but the atmospheric source can also contribute phosphorus to the photic zone, as was shown for the western Mediterranean (Bergametti et al., 1992). Because *E. huxleyi* is an excellent competitor for phosphorus (Riegman et al., 1998), increases in production of this most abundant coccolithophore species are expected in P-controlled systems such as the eastern Mediterranean.

Our work on particle fluxes in Bannock Basin suggests that the productivity pattern could be the result of fertilisation in the upper euphotic zone. The increase in pigment concentration is observed when both wind-induced oceanographic changes from a summer stratified upper water mass to a deep winter mixing (Krom et al., 1992) and wet deposition of Saharan dust occur (compare also Figs. 3.2 and 3.6).

The vertical stability of the water column may play a vital role in determining the productivity of Bannock surface waters. The breakdown of this stability is most important in initiating the late fall increase in plankton production. Coincident with the changes in winds that occur in late fall, surface waters begin to cool and evaporation is highest at this time. Nutrients are scarce in the Mediterranean compared with the rest of the world ocean, because the main input comes from the surface waters of the Atlantic through the Strait of Gibraltar. As a consequence, the central eastern Mediterranean is characterised by an extremely oligotrophic regime (Berland et al., 1988; Dugdale and Wilkerson, 1988).

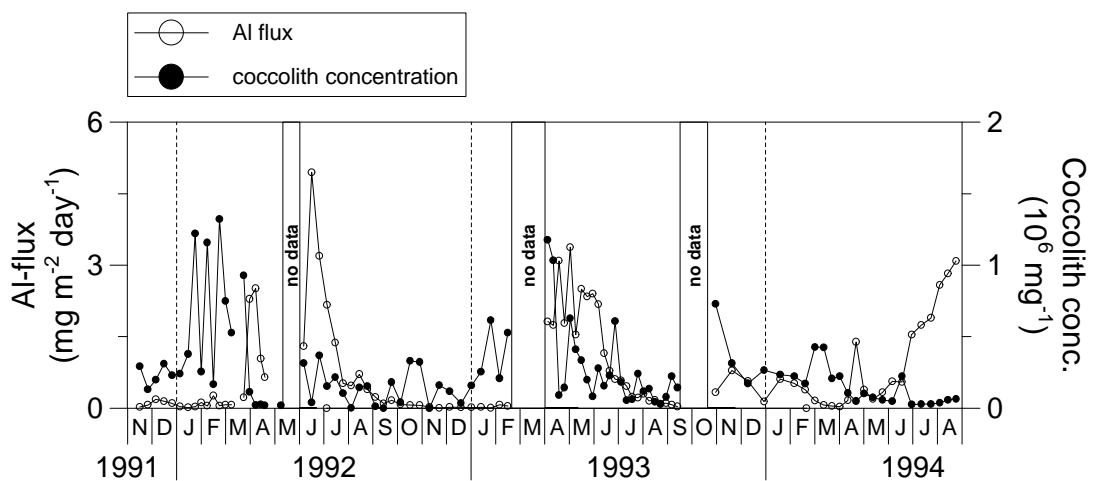


Figure 3.5 Flux record for Al ($\text{mg m}^{-2} \text{day}^{-1}$) and coccolith concentration (number mg^{-1}).

The trap station in Bannock basin is located in the Ionian Sea province of Antoine et al. (1995) in which the winter bloom, as revealed by CZCS, coincides with the breakdown of stratification, and it is of moderate intensity because the nutrient levels are never high. Zohary and Robarts (1998) concluded that phosphorus was the primary limiting nutrient when other factors (such as light and grazing) did not control microbial biomass or activity.

The coccolith and coccosphere sinking rates were calculated from the time lag between

associated pigment maxima at the sea surface (Fig. 3.6) and the coccolith/coccosphere flux maxima in the trap samples and the vertical distance (3000 m). The coccolith sinking rates are very low, ranging from 17 – 25 m day⁻¹ (average time-lag of 4 to 6 months). In contrast, maximum fluxes of coccospheres were recorded mostly from January to April indicating that the time-lag between maximum primary production and maximum export flux at 3000 m water depth was about 1 month. Consequently, it appears that in the eastern Mediterranean, coccospheres sink individually with a rate of approximately 100 m day⁻¹. This settling speed concords with the previous estimations of the sinking speed of particles through the water column (Honjo, 1982; Neuer et al., 1997). Therefore, a possible indicator for primary production in the sediment trap located in the oligotrophic waters of the eastern Mediterranean might be the occurrence of high coccosphere fluxes. However, the contribution of intact coccospheres to the total coccolith flux is relatively small in comparison to the settling flux of individual coccoliths probably associated with small-sized macroaggregates and fecal pellets (considering also that grazing activity and organic matter production is very low in the central eastern Mediterranean). The coccosphere-coccolith flux ratio ranges from 0 to 5.8×10^{-3} (average 5.1×10^{-4}). Individual coccoliths may have been resuspended and redeposited from the shelf into the deep sea, through currents and winds. In contrast, intact coccospheres disintegrate relatively rapidly after the cell dies and are rarely found in sediments. Consequently, the occurrence of coccospheres directly refers to overlying surface water productivity whereas coccoliths may also have a different origin (e.g. compare Figs. 3.2B and 3.2C for January to March 1992).

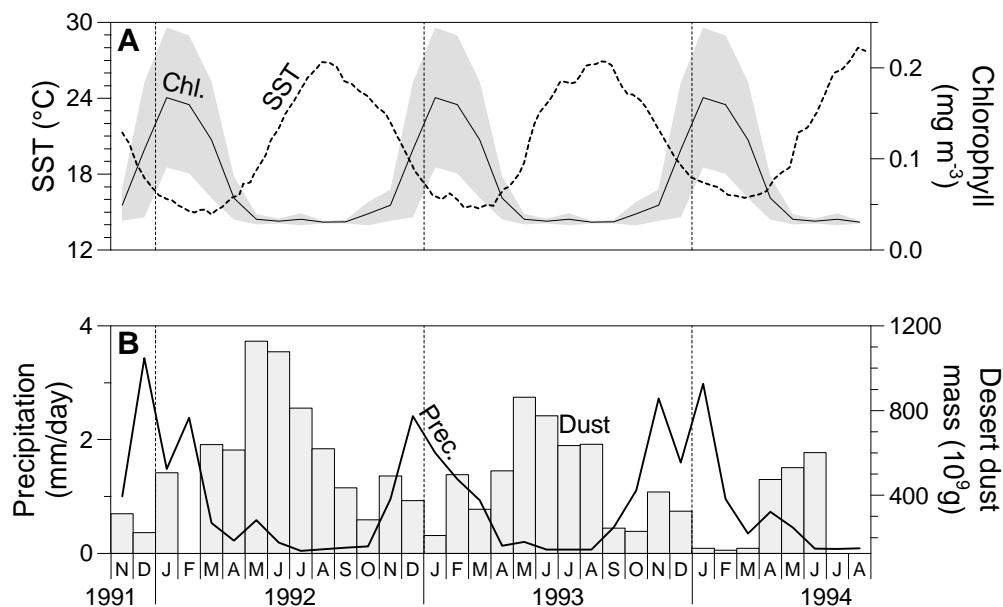


Figure 3.6 Satellite observations: A) Monthly averaged pigment concentrations observed for the period 1979 to 1985 derived from CZCS data (solid line) at the trap location, with the gray area indicating the 1 σ standard deviation for each month, and the weekly composite AVHRR sea surface temperature record at the trap location during the deployment period (dashed line). B) Precipitation at the trap location (line) and desert dust mass over the Mediterranean (bars) during the deployment period. The dust data were redrawn after Dulac et al. (1996).

3.4.3 Flux patterns of *Coccolithophore* species

The most abundant and cosmopolitan coccolithophorid species, *Emiliana huxleyi*, largely dominates the observed assemblage of the fifty coccolithophore species recorded in the trap samples (38 heterococcolith and 12 holococcolith species; Fig. 3.3; Tables 3.3, 3.4). The seasonal trend recorded in coccolith species fluxes is mainly driven by changes in the flux of this species, a dominance of this species already observed in the Mediterranean surface waters by Knappertsbusch (1993) and Kleijne (1993).

The high correlation ($r = 0.90$) between *E. huxleyi* and the deep-dwelling species *Florisphaera profunda* suggests coccolithophore production throughout the water column. *F. profunda* is restricted to the lower euphotic zone in low-middle latitude regions (Okada and Honjo, 1973), and changes in the *F. profunda* abundance through time have been used as a proxy to model palaeonutricline dynamics (Molfino and McIntyre, 1990). The inverse relationship between the *F. profunda* flux and the diatom export production shows that *F. profunda* is inversely related to the intensity of upwelling (Jordan et al., 1996; Ziveri and Thunell, 2000). The relative abundance of *F. profunda* in the coccolith assemblages of eastern Mediterranean sapropelitic sediments has been used to infer palaeonutricline dynamics (Castradori, 1994).

Coccolith fluxes of *Helicosphaera carteri* and *Calcidiscus leptoporus* show a similar seasonal trend ($r = 0.79$) and abundance (Fig. 3.3). This similarity was previously observed in the Quaternary sediments from the North Atlantic and in sediment trap samples from the Southern California Bight and Gulf of California (Gard, 1989; Ziveri et al., 1995, Ziveri and Thunell, 2000). In the Southern California Bight, the highest fluxes of the two species were associated with low to intermediate nutrient concentrations prior to upwelling when total coccolithophore productivity was high. In the Gulf of California both species tend to decrease when the zooplankton grazing pressure increases.

The *Syracosphaera* spp. fluxes represent all of the *Syracosphaera* species recorded in Bannock Basin except *S. pulchra* and *S. histrica*, which have a very low abundance in our samples. The fluxes of *Syracosphaera* spp. show a seasonal signal comparable to *C. leptoporus* and *H. carteri* (Fig. 3.3). The remaining coccolithophore species account for approximately 3.7% of the total assemblage. *Umbellosphaera tenuis* and *U. irregularis* have seasonal trends similar to that of *H. carteri* (Fig. 3.3). Both species are typical of warm, tropical-subtropical waters (McIntyre et al., 1970). The Rhabdosphaeraceae represents only a small part of the species recorded in the present study and are present as *D. tubifera* and *R. clavigera* ad *R. xiphos*. Okada and McIntyre (1979) have described *D. tubifera* and *R. clavigera* as warm water species of the upper water layers. These two species have a subtropical temperature preference, of which *R. clavigera* (3 – 29°C) has a wider temperature range than *D. tubifera* (optimum 21 – 29°C; total range 14 – 30°C). *D. tubifera* is more abundant in oligotrophic water conditions, occurring outside the upwelling areas and has also been described in the warmer areas of the eastern Mediterranean (Kleijne, 1993). In our study, *D. tubifera* is always less than 3% of the coccolith assemblage, but is remarkable in that the increase in both fluxes and relative abundance during the last sampling year (1994) is associated with a low coccolith flux and SST being a few degrees higher than the previous

sampling years. *Scyphosphaera apstenii*, *Umbellosphaera tenuis* and holococcoliths show the same increase during 1994.

3.4.4 Comparison of sediment trap and surface sediment results (Pl. 3.1 and 3.2)

The importance of coccolith calcite in the eastern Mediterranean deep-sea sediments has been established previously (Bernard & Lecal, 1953; Milliman and Muller, 1973). Coccolithophores are the most abundant primary producers that are being preserved in surface sediments in the eastern Mediterranean. This is confirmed by our results on particle fluxes in Bannock Basin, where coccoliths constitute the major part of the biogenic component.

The coarse-size fraction of the biogenic particle flux, including foraminifers, pteropods, and radiolarians, has not been quantified in the trap samples. However, during the analyses of the complete fraction aliquot under both binocular microscope (400×) and LM, it was noted that this fraction was consistently very low. In Bannock Basin, coccolithophores are the dominant phytoplankton group that manufactures a skeleton, and together with calcareous dinoflagellates (mainly *Thoracosphaera heimii*) are also the major contributors to the biogenic carbonate flux. In contrast, in the surface sediment, the >32 µm fraction constitutes approximately 25% of the bulk sediment and contains about 75% biogenic carbonate (mainly foraminifers and pteropods; Plate 3.2) (Chapter 2).

There is no evidence of carbonate dissolution in the trap samples collected at 3000 m water depth in Bannock Basin. The preservation of delicate coccoliths such as *Oolithothus fragilis*, *Discosphaera tubifera* and *Umbilicosphaera* spp. (Roth and Berger, 1975; Schneidermann, 1977) is very good. Perfectly preserved spines of foraminifers were also detected suggesting a good carbonate preservation.

The rest of the flora consists of diatoms and silicoflagellates. They show a flux pattern similar to coccoliths (Ziveri et al., in prep.). The fauna is poorly represented by radiolarians and planktic foraminifers, the latter mainly as juvenile forms. The occurrence of mainly juvenile foraminifers is probably due to the combination of two factors. Firstly, extremely oligotrophic conditions seriously hampers heterotrophic production in the eastern Mediterranean (Turley, 1997). Secondly, the small size of juvenile foraminifers (approximately 20 – 60 µm) allows for easy lateral transport from higher production areas to the Bannock Basin site.

The carbonate content of sediment trap samples and surface sediment samples shows large regional variations. The carbonate content in the trap resembles that found in boxcore MT-6, but is much lower than in the other boxcores. Aluminium correlates inversely with coccolith concentrations (coccoliths mg⁻¹), suggesting the dilution of coccolith carbonate by terrigenous input (Fig. 3.5).

The annual coccolith flux obtained by the sediment trap at 3000 m is comparable to the coccolith accumulation rates of the aerobic surface sediment of boxcore UM15 and is about one third of the coccolith accumulation rate calculated in the anaerobic surface sediment of Bannock Basin (MT6) (Fig. 3.4). Differences with a similar order of magnitude have been obtained by the comparison of the coccolith fluxes in the two traps in the aerobic (this chapter) and anaerobic water conditions (Ziveri et al., 1996). The main difference

between the coccolith assemblages of sediment trap and surface sediment samples is the presence of *Reticulofenestra* “overcalcified” sp. in the surface sediment. Because this species has a very low abundance in the sediment trap, we conclude that, in combination with the same trend for the large-size fraction (high in surface sediments, low in the sediment trap), the long-term variability in faunal and floral assemblages is not captured by the sediment trap, possibly due to irregular blooms (see also Chapter 2).

3.5 Summary and conclusions

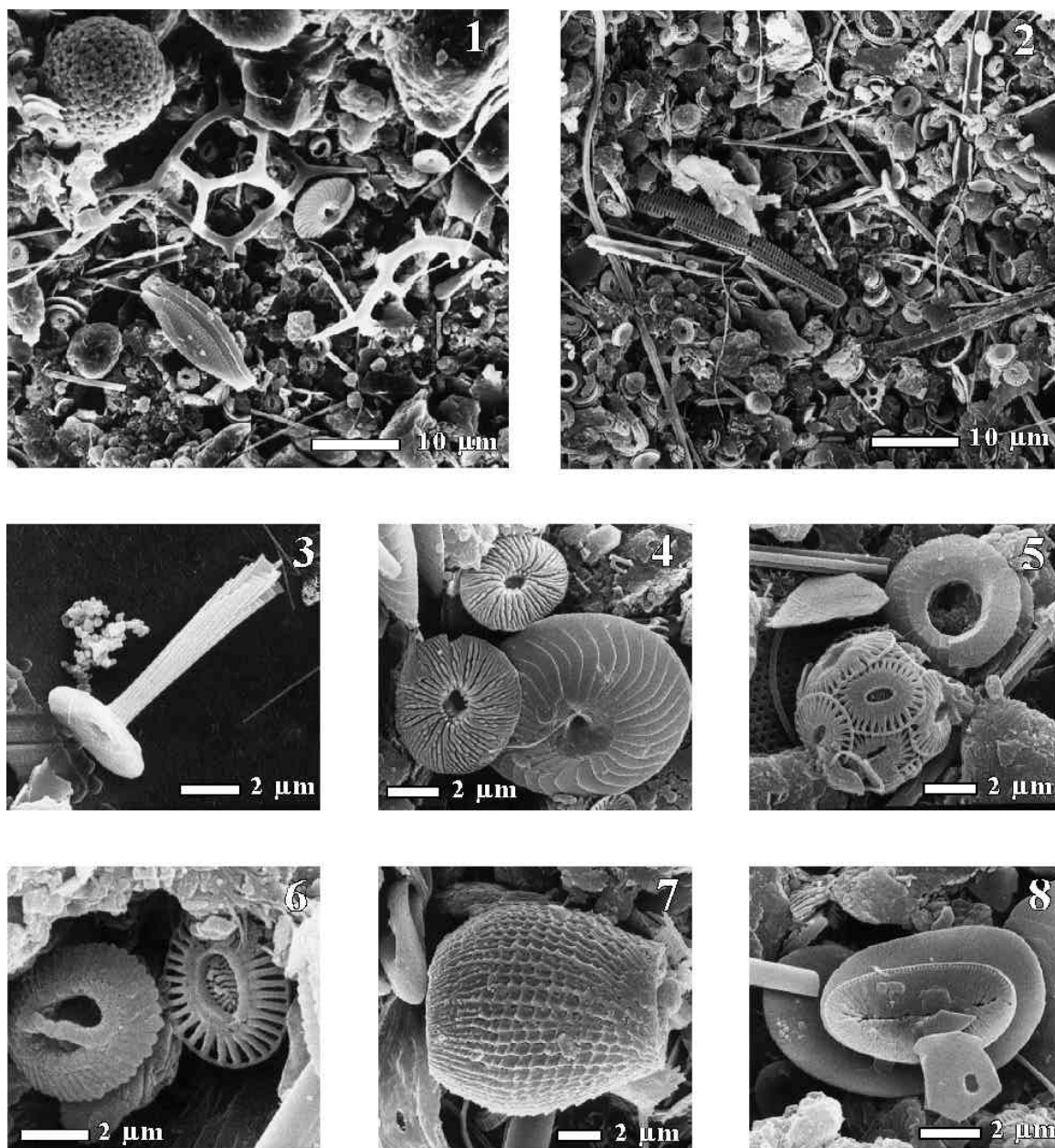
This work, concentrating on coccolithophores and thoracosphaerid fluxes as the major contributors to the biogenic carbonate flux recorded at 3000 m in the oligotrophic waters of the central eastern Mediterranean Sea, has shown that:

1. A strong seasonal variation in the total mass flux is recorded by the total coccolith and coccosphere flux, with maximum fluxes occurring in late winter and spring.
2. The annual coccolith flux of 1.0×10^{10} coccoliths $\text{m}^{-2} \text{yr}^{-1}$ measured in the deep waters at 3000 m water depth is much lower than most published data recorded in other oceanographic settings, even when corrected for the trap efficiency (23%).
3. The biogenic and lithogenic fluxes are primarily controlled by coccoliths and Saharan dust input, respectively.
4. The calculated coccolith and coccosphere settling speeds estimated from the comparison of maximum pigment concentration at the sea surface and maximum flux at 3000 m water depth were 17 to 25 m day^{-1} for coccoliths and 100 m day^{-1} for coccospheres.
5. *Emiliania huxleyi* and *Florisphaera profunda*, followed by *H. carteri* and *C. leptoporus*, are the dominant coccolith species in sediment trap samples as well as surface sediments. *Reticulofenestra* “overcalcified” sp. is a major species in the surface sediments only. This anomaly is comparable to that observed for the large-size ($>32 \mu\text{m}$) fraction, which is nearly absent in the sediment trap, but abundant in surface sediments. Both might be related to long-term differences in faunal and floral assemblages, possibly due to irregular blooms.

Acknowledgements – P.J.M. van Santvoort, G. Nobbe and H. de Waard are thanked for their analytical assistance. We are grateful to Agostino Rizzi, (University of Milan) and Saskia Kars (Vrije Universiteit Amsterdam) for operating the SEM. The chapter benefited greatly from comments by E. Erba and R. Thunell. The pigment data are courtesy of the Joint Research Centre (European Commission / European Space Agency). The SST data were extracted from the Weekly NCEP SST Database at the NOAA/WRC Server *Ferret* and the precipitation data from the GPCP Global Combined Precipitation Dataset (part of the Climatology Interdisciplinary Data Collection). This study was supported by MARFLUX (MAST1-90022C), PALAEOFLUX (MAS2-CT93-0051) and SAP (MAS3-CT97-0137) European programmes.

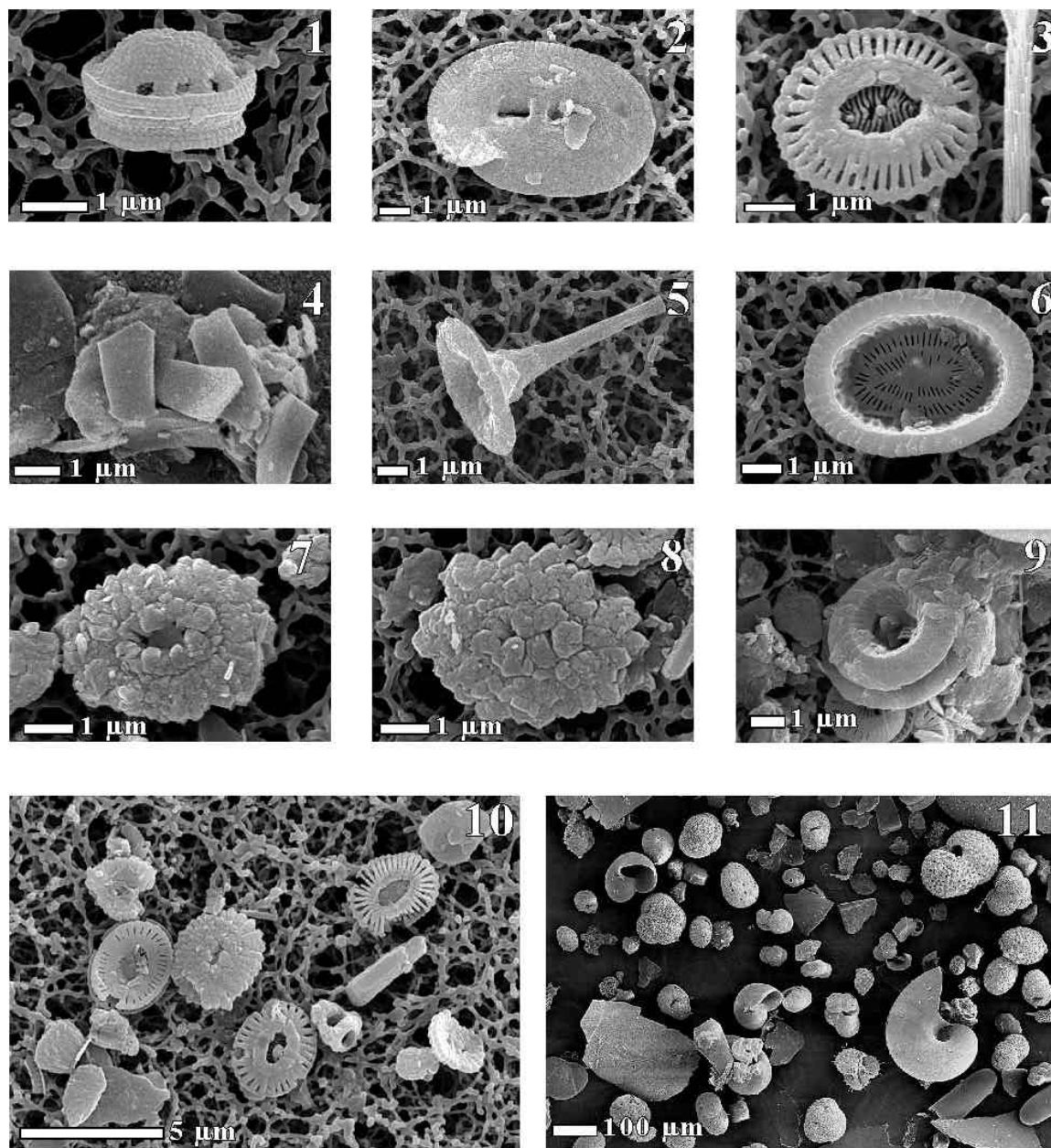
This is Netherlands Sedimentary Research School (NSG) contribution 990309.

Plate 3.1 Sediment trap samples



1. Assemblages of sample MT4O-1
2. Assemblages of sample MUB-1
3. *Rhabdosphaera clavigera* var. *clavigera*, rhabdolith, (sample MT4O-18)
4. *Umbilicosphaera tenuis*, umbelloliths, and *Calcidiscus leptoporus*, distal view of the distal shield, (sample MT4O-16)
5. *Emiliana huxleyi*, coccosphere, and *Umbilicosphaera sibogae*, distal view of the distal shield, (sample ST2-20)
6. *Emiliana huxleyi* and gephyrocapsid, distal view of the distal shields (sample MT4O-1)
7. *Syracosphaera apstenii*, lopadolith, (sample MUB-10)
8. *Helicosphaera carteri*, proximal view of coccolith, and *F. profunda*, coccolith, (sample MUB-1)

Plate 3.2 Surface sediment samples



1. *Calyptosphaera pirus*, areolith, (sample UM15 <32 μm)
2. *Helicosphaera carteri*, distal view, (sample UM35 <32 μm)
3. *Emiliania huxleyi*, distal view, (sample UM26 <32 μm)
4. *Florisphaera profunda* coccoliths, (sample MT6)
5. *Discosphaera tubifera*, rhabdolith, (sample UM35)
6. *Syracosphaera pulchra*, cancolith, distal view, (sample UM35)
7. *Reticulofenestra* “overcalcified” sp., distal view, (sample UM26 <32 μm)
8. *Reticulofenestra* “overcalcified” sp., distal view, (sample UM26 <32 μm)
9. *Umbilicosphaera sibogae*, distal view, (sample UM15 <32 μm)
10. Assemblages of sample UM15 <32 μm
11. Assemblages of sample UM15 >32 μm

Appendix 3-A

The anoxic boxcore MT6 has an almost ideal ^{210}Pb profile (Fig. 3-A.1) from which the mass accumulation rate can be determined. Mean porosity is taken into account in the boxcore for the calculation of the average linear sedimentation rate from the mass accumulation rate. The determined mass accumulation rate is $166.0 \text{ mg m}^{-2} \text{ day}^{-1}$. The average dry bulk density is 0.429 g cm^{-3} . Dividing the mass accumulation rate by the dry bulk density gives an average linear sedimentation rate of 14.1 cm kyr^{-1} .

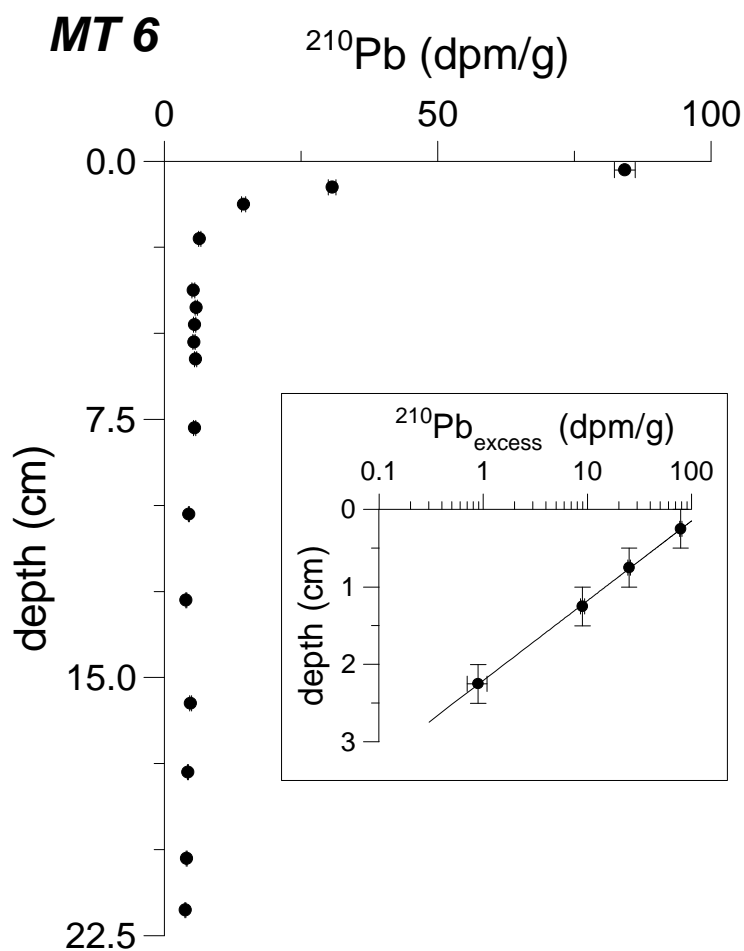


Figure 3-A.1 Pb-210 (dpm/g) vs. depth in boxcore MT6.

